ARMY RESEARCH LABORATORY

Wave Dispersion in Cylindrical Tubes: Applications to Hopkinson Pressure Bar Experimental Techniques

by Libo Ren, Mike Larson, Bazle A. Gama, and John W. Gillespie, Jr.

ARL-CR-551 **September 2004**

prepared by

Center for Composite Materials
University of Delaware
Newark, DE 19716

under contract

DAAD19-01-2-0005

NOTICES

Disclaimers

Army Research Laboratory

Aberdeen Proving Ground, MD 21005-5069

ARL-CR-551 **September 2004**

Wave Dispersion in Cylindrical Tubes: Applications to Hopkinson Pressure Bar Experimental Techniques

Libo Ren, Mike Larson, Bazle A. Gama, and John W. Gillespie, Jr.
Center for Composite Materials
University of Delaware

prepared by

Center for Composite Materials
University of Delaware
Newark, DE 19716

under contract

DAAD19-01-2-0005

REPORT DOCUMENTATION PAGE			*Form Approved* *OMB No. 0704-0188*

1. REPORT DATE *(DD-MM-YYYY)*	**2. REPORT TYPE**	**3. DATES COVERED (From - To)**
September 2004	Final	January 2003–April 2003

4. TITLE AND SUBTITLE
Wave Dispersion in Cylindrical Tubes: Applications to Hopkinson Pressure Bar Experimental Techniques

5a. CONTRACT NUMBER
DAAD19-01-2-0005

5b. GRANT NUMBER

5c. PROGRAM ELEMENT NUMBER

6. AUTHOR(S)
Libo Ren,* Mike Larson,* Bazle A. Gama,* and John W. Gillespie, Jr.*

5d. PROJECT NUMBER
622618.AH80

5e. TASK NUMBER

5f. WORK UNIT NUMBER

7. PERFORMING ORGANIZATION NAME(S) AND ADDRESS(ES)
University of Delaware
Center for Composite Materials
Newark, DE 19716

8. PERFORMING ORGANIZATION REPORT NUMBER

9. SPONSORING/MONITORING AGENCY NAME(S) AND ADDRESS(ES)
U.S. Army Research Laboratory
ATTN: AMSRD-ARL-WM-MB
Aberdeen Proving Ground, MD 21005-5069

10. SPONSOR/MONITOR'S ACRONYM(S)
ARL-CR-551

11. SPONSOR/MONITOR'S REPORT NUMBER(S)

12. DISTRIBUTION/AVAILABILITY STATEMENT
Approved for public release; distribution is unlimited.

13. SUPPLEMENTARY NOTES
*University of Delaware, Center for Composite Materials, Newark, DE 19716

14. ABSTRACT
It is well known that harmonic waves with higher frequencies travel slower than those with lower frequencies and that they are known as “wave dispersion” in finite diameter rods. From the frequency equation, the phase speed can be determined if the wavelength is known. A dispersion correction methodology uses the frequency equation to disperse a waveform to a specific location of interest. Dispersion correction methodologies are generally used in split-Hopkinson pressure bar (SHPB) techniques to reduce experimental data accurately. This report investigates wave propagation and wave dispersion in cylindrical tubes. Based on the work of Mirsky and Herrmann (M-H), the phase speed can be solved for wave motion along a cylindrical tube with a specific thickness-to-radius ratio. A numerical algorithm is developed to solve the M-H model and is compared with the solutions obtained from a three-dimensional finite element model. It is found that the first mode of the M-H solution gives the correct phase speed for wave motion in a tube. A modification to the traditional inverse fast Fourier transform algorithm is proposed for better prediction of the dispersed signal. The effects of the tube dimensions and the accuracy of dispersion correction in SHPB experiments are also discussed.

15. SUBJECT TERMS
wave dispersion, split-Hopkinson pressure bar experiment, cylindrical tubes

16. SECURITY CLASSIFICATION OF:			**17. LIMITATION OF ABSTRACT**	**18. NUMBER OF PAGES**	**19a. NAME OF RESPONSIBLE PERSON**
					Libo Ren
a. REPORT	**b. ABSTRACT**	**c. THIS PAGE**			**19b. TELEPHONE NUMBER** (*Include area code*)
UNCLASSIFIED	UNCLASSIFIED	UNCLASSIFIED	UL	42	302-831-0248

Standard Form 298 (Rev. 8/98)
Prescribed by ANSI Std. Z39.18

Contents

List of Figures

Acknowledgments

This report is prepared through participation in the Composite Materials Technology Collaborative Program sponsored by the U.S. Army Research Laboratory under Cooperative Agreement DAAD09-01-2-0005. Libo Ren would like to thank Dr. J. R. Xiao and Dr. Y. P. Duan at the University of Delaware-Center for Composite Materials for helpful discussions on wave propagation theory.

INTENTIONALLY LEFT BLANK.

1. Introduction

The split-Hopkinson pressure bar (SHPB) experimental technique has become a standard method in determining the dynamic mechanical properties of materials. The Hopkinson pressure bar technique was originally developed by B. Hopkinson (*1*) in 1914 to measure the pressure generated by the detonation of explosives. In 1948, R. M. Davies (*2*) conducted a critical study of the Hopkinson pressure bar technique. He developed the axial and radial strain measurement system and analyzed the wave dispersion effects. In 1949, H. Kolsky (*3*) invented the SHPB technique. In his work, he used the same system as Davies' to measure the strain. At the same time, he developed a one-dimensional (1-D) model to perform experimental data analysis. The work of Hopkinson, Davies, and Kolsky established the foundation for the development of the SHPB technique. Figure 1 shows a classic SHPB test setup, which consists of one striker bar (SB), one incident bar (IB) and one transmission bar (TB), equal in diameter and usually made from the same material. Strain gages are mounted on the surfaces of IB (SG1) and TB (SG2) to record the strain. The specimen (SP) is sandwiched between the IB and the TB. The SB, powered by pressured gas, will hit the IB. A compressive stress wave will travel along the IB and reach the IB-specimen (IB-S) interface. At this interface, one part of it will be reflected back into IB, and the rest will be transmitted to the TB through the specimen-transmission bar (S-TB) interface. The strain gage SG1 will record two waves: incident wave and reflected wave and the strain gage SG2 will record only the transmitted wave. Data reduction on these three waves will provide the stress-strain response of the specimen material under dynamic loading.

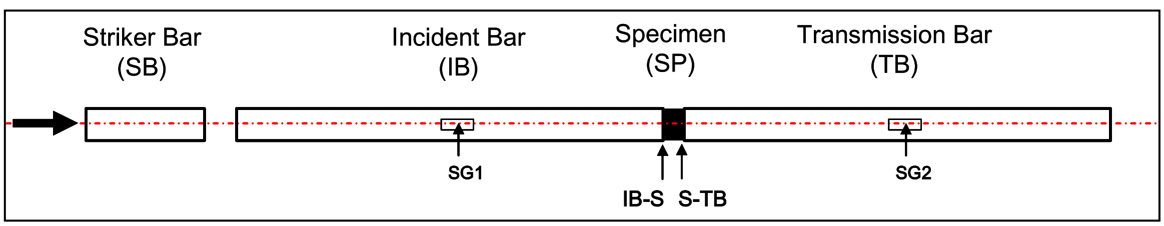

Figure 1. Schematic diagram of SHPB setup.

The classical SHPB data analysis is based on 1-D wave propagation theory in long rods. Several assumptions have been made for the 1-D theory. Two important assumptions are as follows: (1) stress wave propagation in the bars is 1-D, and (2) the bars are free of dispersion effects. Actually, these two assumptions are not satisfied for finite diameter bars. Based on such assumptions, the strain data measured at the middle point of the bars are directly used as the strain at the interfaces to reduce the data. Strictly speaking, wave propagation in cylindrical bars is three-dimensional (3-D) in nature: both axial and radial stresses, and strains are generated when the stress wave travel along the bar. Such variables are functions of radial dimension, so they are not uniform across the cross section. The wave dispersion effect exists, which means that the harmonic wave with higher frequencies travels more slowly than the wave with lower frequencies. Due to this effect, the wave shape keeps changing as it travels along the axial direction. This effect should be considered for accurate data reduction.

Many authors have investigated the wave dispersion effect in order to modify the classical 1-D data analysis algorithm. Their study is based on the work of Pochhammer (*4*) and Chree (*5*), who independently solved the problem of wave propagation in an infinite cylindrical rod with finite diameter and derived the frequency equation. This frequency equation establishes the relationship between phase velocities and wavelengths of harmonic waves. Later Davies (*2*) and Bancroft (*6*) solved the equation numerically for some limiting cases. With the help of modern computers, the frequency equation can be easily solved over the complete range of geometric and material parameters. Follansbee and Frantz (*7*) and Gong et al. (*8*) investigated the effect of wave dispersion correction for the SHPB test and found that significant improvement on the stress-strain data can be achieved by wave dispersion correction. During dispersion correction, Fourier transformation (FT) is used to decompose the measured strain data into its harmonic waves. The dispersion correction methodology is then applied for each component frequencies. Finally, inverse FT is performed to get the dispersed wave at the IB-S and S-TB interfaces. Other dispersion correction methods were also suggested, e.g., in Li and Lambros (*9*). Currently wave dispersion correction has become a standard procedure in SHPB data analysis.

In this report, the wave dispersion in cylindrical tubes for the SHPB application is investigated. This study has become important and indispensable because recently cylindrical tubes have been used for SHPB experiments. For example, Dowling et al. (*10*) performed a dynamic punch shear test to study the mechanical properties of metals. This technique uses a transmission tube in place of the TB, such that the IB can shear a cylindrical disc through the specimen. This test method is still being extensively used today. Another example is determining the mechanical properties of low-strength, low-impedance materials under dynamic loading. If solid TBs are used for the SHPB test, the noise level is so high that proper interpretation of the transmission signal becomes impossible. To solve this problem, some researchers have used visco-elastic bars e.g., see Zhao et al. (*11*). The disadvantage of using visco-elastic bars is that additional assumptions have to be made about the visco-elastic material properties, which may not represent the true characteristics of the bar materials at high strain rates. Furthermore, the material properties are functions of temperature, moisture, and aging conditions, which are difficult to control. In addition, the dispersion correction algorithm now becomes very extensive and time consuming due to the visco-elastic nature of the bar materials. Other researchers have put forward the idea of using a hollow cylindrical tube for the transmission part of the SHPB test. Recently, Chen et al. (*12*) used IB and transmission tube made of high-strength Al alloy to measure the dynamic mechanical properties of silicon (Si) rubber materials. In this way, they obtained higher amplitude transmission signal that was achievable using a solid bar. The problem is that they did not perform any dispersion correction on the incident and transmission signals, which were collected from midpoints of the bar/tube. They used pulse shaper to filter the high-frequency components in the waveform and then claimed that dispersion correction was not necessary. This argument is not correct because the same argument can be applied to the traditional SHPB test, which means if pulse shaper is used, dispersion correction is not necessary any longer. It is not clear how to define the lower limit of high-frequency wave components without a dispersion correction methodology. The use of a pulse shaper can improve the result but cannot eliminate the necessity of dispersion correction. It is still necessary to investigate the wave propagation in a cylindrical tube and find the appropriate dispersion relations, and is the objective of the present study.

Wave propagation in infinitely long tubes has been discussed by several authors, as early as in the 1920s. Ghosh (*13*) studied the longitudinal motions of a hollow cylinder with 3-D theory. In 1952, Fay (*14*) investigated this problem again and derived the frequency equation. But there was an error in his equation, which was pointed out by Herrmann and Mirsky (*15*). The work of Mirsky and Herrmann (M-H model) is considered the most comprehensive treatment (*15, 16*). They used both 3-D theory and shell theory to study the wave motion in cylindrical tube. Using 3-D theory, they derived the exact frequency equation, and their shell theory considered membrane effect, bending effect, transverse shear deformation, and rotary inertia. They claimed that the results of 3-D theory and shell theory were very close.

This study is based on the work of Mirsky and Herrmann (*16*). First, the two frequency equations will be solved again to make sure that the shell theory really gives a solution to phase speed, which is accurate enough. Then the results of M-H shell theory will be applied to the SHPB test. It will be shown that the first mode solution is correct for the SHPB application. A modified dispersion correction algorithm will be suggested to make accurate prediction of strain at the IB-S and at the specimen-transmission tube (S-TT) interfaces. Finally, the effects of the tube geometry on the accuracy of data reduction will be discussed.

2. Solution of M-H Model

As mentioned earlier, Herrmann and Mirsky (*15, 16*) derived the exact frequency equation for cylindrical tubes by solving the 3-D problem and one approximate frequency equation through shell theory. The 3-D theory gave the exact frequency equation in cylindrical coordinates (r, θ, z) (*15*):

$$\begin{aligned} F_{3D}(c, h/\Lambda) = {} & [K_{10}(\beta)K_{01}(\gamma) + K_{01}(\beta)K_{10}(\gamma) + (8/(\pi^2\beta\gamma ab)) \\ & + FK_{11}(\gamma)K_{00}(\beta) + (1/F)K_{11}(\beta)K_{00}(\gamma)] + [(1+\overline{B})^2/(F\gamma^2 ab)]K_{11}(\beta)K_{11}(\gamma) \\ & - [(1+\overline{B})/(\gamma ab)][aK_{11}(\gamma)K_{10}(\beta) + bK_{11}(\gamma)K_{01}(\beta)] \\ & - [(1+\overline{B})/(F\gamma ab)][aK_{11}(\beta)K_{10}(\gamma) + bK_{11}(\beta)K_{01}(\gamma)] = 0\,, \end{aligned} \qquad (1)$$

where

$$K_{mn}(z) = J_m(zb)Y_n(za) - J_n(za)Y_m(zb), c_c = \sqrt{(\lambda + 2\mu)/\rho c_s} = \sqrt{\mu/\rho}$$

and

$$\beta^2 = \alpha^2(\frac{c^2}{c_c^2} - 1), \gamma^2 = \alpha^2(\frac{c^2}{c_s^2} - 1), \overline{B} = (\frac{c^2}{2c_s^2} - 1),\ F = \frac{\alpha^2 \overline{B}^2}{\beta\gamma}. \qquad (2)$$

In equation 2, α is the wave number $2\pi/\Lambda$ and J_m, Y_m are the Bessel functions, a and b are the inner and outer radii of the tube, λ and μ are Lame's constants, ρ is tube material density. c is the phase speed to be solved, $h = b - a$ is the thickness of the tube wall and Λ is the wave length. Mirsky and Herrmann also derived one approximate frequency equation based on shell theory (*16*). This equation is very lengthy, so it is not listed here. Basically, this equation is in following format:

$$F_{shell}(s, \delta) = A_1(m)(s^2 - M)^2(s^2 - k^2)^2\delta^8 + [A_2(m)s^6 + A_3(m)s^4 + A_4(m)s^2 + A_5(m)]\delta^6$$
$$+[A_6(m)s^4 + A_7(m)s^2 + A_8(m)]\delta^4 - A_9(m)[s^2 - A_{10}(m)]\delta^2 = 0. \qquad (3)$$

where $s = c/c_s$, $\delta = h/\Lambda$, $A_1, , , A_{10}$ and M are constants which are functions of tube geometry parameter $m = h/R$ (*16*), ν is the material Poisson's ratio, k is the shear coefficient in M-H shell model which is related to Poisson's ratio ν (*15*). Here $R = (a + b)/2$ is the mean tube radius. From equation 3, it can be seen that phase speed is a function of both m and δ.

Equation 1 is transcendental in nature but can be solved with the help of mathematical software such as MAPLE or MATHEMATICA. From equation 2, it can be seen that β and/or γ could become imaginary. When $c < c_s$ and $c < c_c$, both β and γ are imaginary. When $c_s < c < c_c$, γ is real but β is imaginary. Wherever one variable becomes imaginary, Bessel function I_m, K_m must be used in place of J_m, Y_m. Such replacement guarantees that the imaginary number i will be eliminated from the equation so that the real roots can be obtained.

Equation 3 can be solved easily using the Newton-Raphson method. There are four real solutions. When the wavelength is very long, δ approaches zero and the first and second solutions of s approach the shear coefficient k. This coefficient k leads numerically to the same phase speed as the limiting solution for wave speed in cylindrical rods when the wavelength approaches infinity. So it is interesting to see that M-H shell model explains the physical meaning of this limiting solution.

The solutions of equations 1, 2, and 3 for various tube geometries are shown in figure 2. There are infinite solutions for the frequency equations. Here, only the first-mode solutions are shown. The following material constants are assumed: $E = 206.09\ \text{GPa}$, $\rho = 7850\ \text{kg/m}^3$, and Poisson's ratio $\nu = 0.30$. It can be seen that the two models provide very close solutions. The maximum difference occurs at the "valley" of the curves. As an example, for $m = 0.250$, 3-D

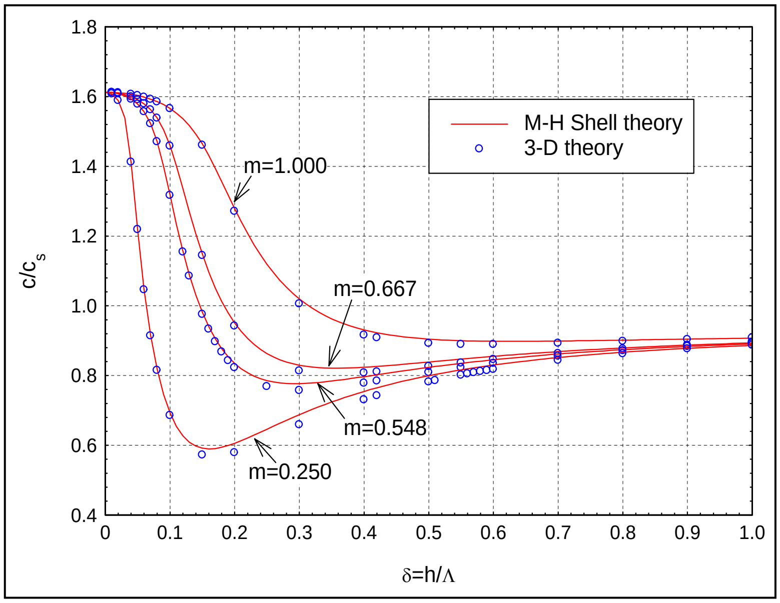

Figure 2. Solution of the frequency by 3-D theory and shell theory for various *m* values.

theory gives $c/c_s = 0.5720$, shell theory gives $c/c_s = 0.5916$, and the error is ~3%. This error is 0.54%, 0.29%, 0.21% for $m = 0.548$, $m = 0.667$ (2/3) and $m = 1.000$, respectively. The error decreases when *m* increases. Figure 3 shows the solutions by shell theory for various *m* values. When $m = 0.033$ (1/30), the phase speed decreases very quickly over the range of low δ. With increasing *m*, the phase speed drops more slowly with δ. There exists one minimum (valley) point for all the curves, after which speed starts to increase. It is obvious that all the curves approach to one limiting speed when δ goes to infinity. For the material properties used here, this limiting phase speed is $0.927\,c_s$.

One important observation from phase speed solutions is that the general claim "wave components with lower frequencies travel faster than wave components with higher frequencies," which is always true for the cylindrical rod, does not always hold true for the cylindrical tubes. For small m values, the phase speed first drops then increases. When m becomes higher, the claim may hold for the whole range of δ.

On the other hand, in this study, it will be shown that the phase speed will not fall into the range where phase speed increases with δ. When we discuss the results later, for simplicity, we still use the claim that the lower frequency wave moves faster.

Bancroft (*6*) solved the frequency equation for the cylindrical rod. He gave the value of c_k / c_c when δ approaches infinity. Herrmann and Mirsky (*15*) also gave these values. The comparison is shown in figure 4. It is clear that these two sets of solutions are exactly the same, which also verifies the correctness of M-H models.

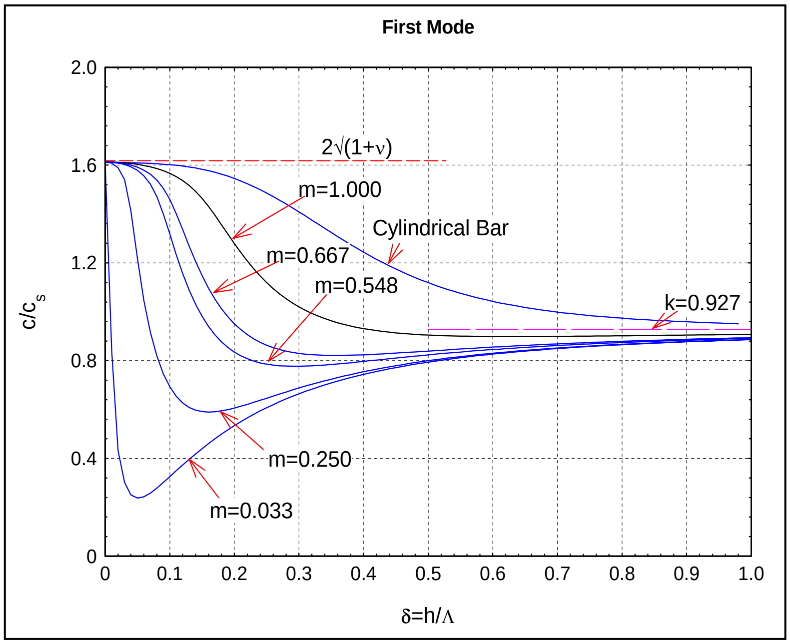

Figure 3. Solution of the frequency equation by shell theory for various m = h/R.

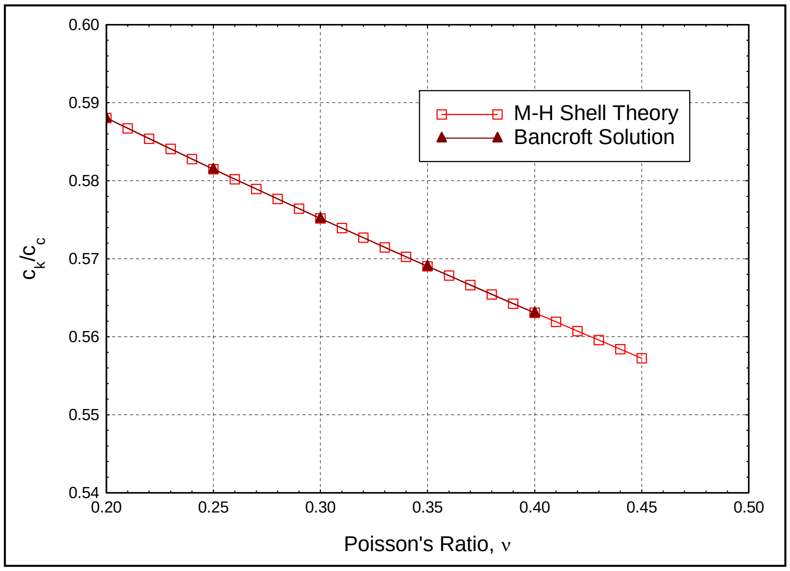

Figure 4. c_k / c_c when $\delta = h / \Lambda$ approaches infinity, $c_c = \sqrt{E / \rho}$.

Now it is proven that the 3-D theory and the shell theory give solutions that can be considered the same. Shell theory solutions will be used for further investigation. The advantage of using the shell theory model is that the frequency equation of the shell model is not transcendental, so it is straightforward to include the model into a computer code.

Mirsky and Herrmann discussed the first-mode solution thoroughly. But they were not sure if wave motion in tubes always follows the first-mode solution, and they did not mention the application of their models to the SHPB experiment either. So it is not clear if the first-mode solution can be used to determine the phase speed in the SHPB experiments. Follansbee et al. (*7*) proved that the solid cylindrical bars in the SHPB experiment vibrate in the first mode, so it may also be true for the hollow cylindrical tubes. To prove this assumption, 3-D finite element analysis is performed to simulate the wave motion in the tubes and is compared with the shell theory for the first mode.

3. Modification of Traditional Dispersion Algorithm

3.1 Solution of Phase Speed

In predicting the dispersed waveform by M-H shell model, the first step is to determine the phase speed of every harmonic wave component. Another equation is required in addition to the $c/c_s \sim h/\Lambda$ relationship shown in figure 3:

$$2\pi(c/c_s)\cdot(h/\Lambda) = k\omega_0(h/c_s), \tag{4}$$

which is equivalent to

$$c(k) = f(k)\,\Lambda = (k\omega_0/2\pi)\cdot\Lambda\,. \tag{5}$$

Here, $k = 1,,,K = N/2$ and N are the numbers of strain data collected by the strain gages. Phase speed $c(k)$ can be solved by finding the intersection of the two curves represented by equations 3–5 numerically. Felice (*17*) performed nonlinear fitting on the solution of frequency equation for cylindrical rods to obtain one explicit relationship between c/c_s and h/Λ. Then it was easy to use this relationship and equation 4–5 together to determine the phase speed. For cylindrical tubes, this fitting method does not work because the shape of the $c/c_s \sim h/\Lambda$ curves changes significantly with *m* as shown in figure 3. On the other hand, the nonlinear fitting is not necessary. This is because there is one implicit functional relationship between c/c_s and h/Λ in equation 3. Giving one h/Λ value, the first-mode solution c/c_s can be determined numerically from equation 3. With the help of this observation, the phase speed of wave components can be determined using equations 3 and 4.

3.2 Reconstruction of Waveform

A modification is suggested in this study on dispersion correction. In traditional dispersion correction algorithm, the following equation is used to reconstruct the waveform:

$$f(t) = \frac{A_0}{2} + \sum_{k=1}^{N/2}[A_k\cos(k\omega_0 t') + B_k\sin(k\omega_0 t')]\,, \tag{6}$$

with

$$t' = t - \Delta z\left(\frac{1}{c_k} - \frac{1}{c_0}\right). \quad (7)$$

Here, A_0, A_k, and B_k are the coefficients of harmonic wave components determined by Fourier transform (FT). Δz is the distance between the strain gage and the destination position. c_k is the phase speed of the wave with frequency $k\omega_0$. This modification is explained in figure 5. Suppose there are two sinusoidal waves sin(t) and sin(2t) traveling together in a tube. At location A, the two waves are in phase. Now let them travel forward to location B. Because the wave with higher frequency travels slower than the wave with lower frequency, wave sin(t) will arrive at location B earlier (at time T_1) than sin(2t) (at time T_2). From time T_1 to time T_2, the contribution from wave sin(2t) to stress and strain at location B should be zero because it has not arrived yet. In the traditional algorithm, the stress and strain response is taken to be $\sin(2(t- L_{AB}/c_2+L_{AB}/c_0))$, where L_{AB} is the distance between location A and location B, c_2 is the phase speed for sin(2t), and c_0 is the fundamental speed.

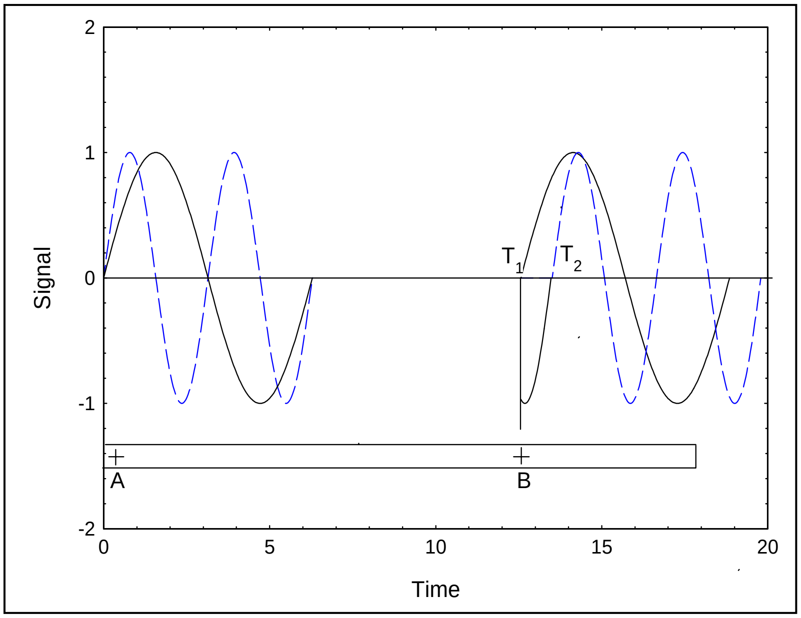

Figure 5. Explanation of new dispersion algorithm for SHPB.

Based on this observation, the algorithm for inverse fast Fourier transform (FFT) in SHPB application should be modified. Suppose the initial time the signal arrives at one certain position is $t = 0$. At time $t = tx$, the signal should be reconstructed as in the following pseudocode:

Signal: $= A_0/2.0$;

For $k = 1$ to N/2

If (tx<($\Delta z / c_k$ - $\Delta z / c_0$))

Do nothing;

Else

$$\text{Signal} \Leftarrow \text{Signal} + A_k \cos(k\omega_0 (tx - \Delta z / c_k + \Delta z / c_0)) + B_k \sin(k\omega_0 (tx - \Delta z / c_k + \Delta z / c_0));$$

The higher frequency wave travels slower than the lower frequency wave. The lower frequency wave reaches location B at time T_1. No response should be generated by the higher frequency wave at location B until after time T_2.

After the coefficients A_0, A_k, and B_k are determined, this modified dispersion algorithm is applied to each harmonic component in reconstructing the waveform.

4. Finite Element (FE) Analysis

FE analysis was performed to check the prediction of the M-H shell model. Stress wave propagation in two cylindrical tubes was simulated. These tubes have $m = h / R$ values of 0.548–0.667. The dimensions of the tube with $m = 0.548$ are as follows: inner radius $a = 7.24$ mm, outer radius $b = 12.7$ mm, and the length is $L = 1.524$ m. Tubes with such dimensions are commercially available and suitable for Hopkinson bar applications. The dimensions of the tube with $m = 0.667$ are as follows: inner radius $a = 5.46$ mm, outer radius $b = 10.92$ mm, and the length is $L = 1.524$ m. Both tubes have a wall thickness of 5.46 mm. The tube material is modeled as steel with Young's modulus E = 206.09 GPa, Poisson's ratio $\nu = 0.3$, and density $\rho = 7850$ Kg/m^3. A trapezoidal stress pulse is applied at one end of the tube, and the wave propagation in the tube is monitored. The other end is assumed to be traction free, so the stress wave will reflect from that end. Due to the symmetric nature of this problem, only one quarter of the tube is analyzed.

Commercial FE analysis code ABAQUS/Explicit* was used to perform the analysis. Element type C3D8R, which is 8-node brick element with reduced integration, was used to generate the mesh. The numbers of elements along the radial direction, tangential direction, and axial direction are 5, 20, and 600, respectively, with a total of 60,000 elements. These elements are uniformly distributed along the axial direction. Figure 6 shows the model and the mesh generation. The boundary conditions are set as follows: zero *x* displacement along edge $X = 0$; and zero *y* displacement along edge $Y = 0$. Figure 7 defines the trapezoidal stress pulse applied on the end face $Z = 0$. The stress history is defined with several time and stress parameters as described in figure 7. The values used in the present analyses are as follows: $t_A = 0$ µs, $t_B = 25$ µs, $t_C = 35$ µs, $t_D = 105$ µs, $t_E = 115$ µs, $t_F = 140$ µs and $P_{max} = 500$ MPa.

* ABAQUS/Explicit is a registered trademark of Abaqus Inc.

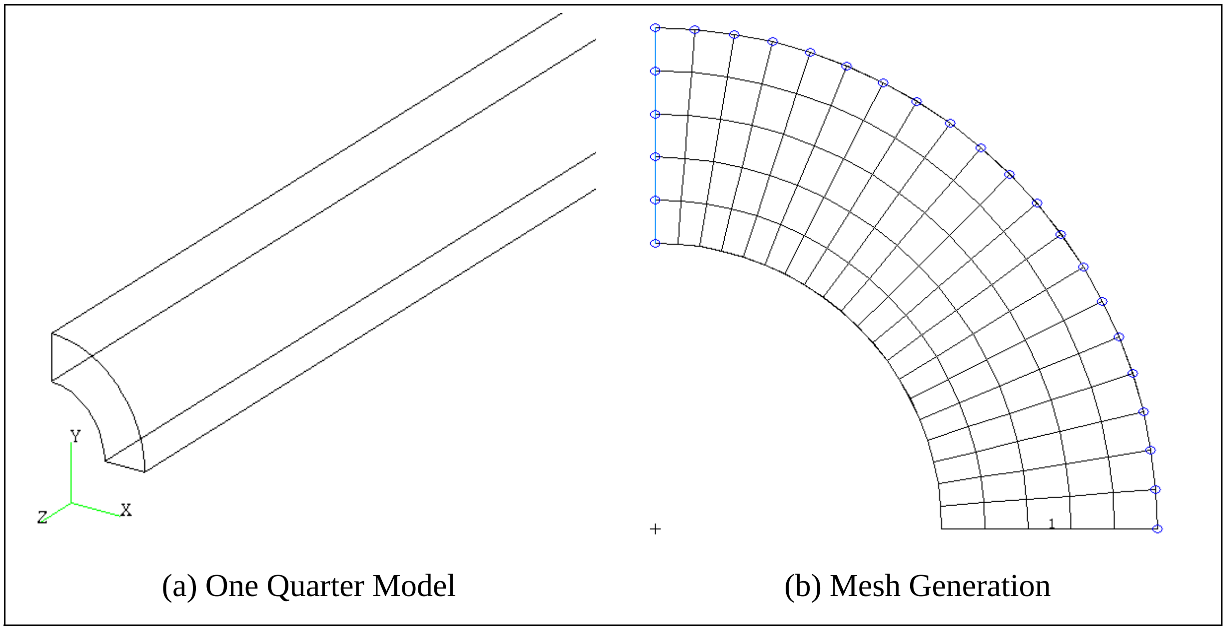

Figure 6. FE model of a cylindrical tube.

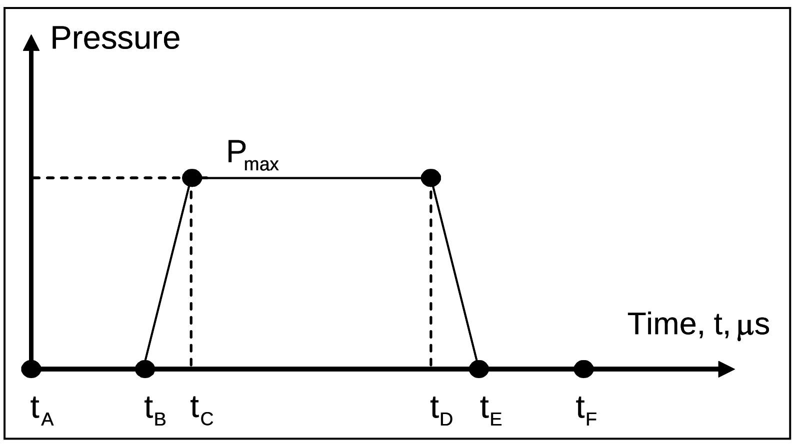

Figure 7. Definition of stress wave applied on the end surface of the cylindrical tube.

Figure 8 gives the strain history at the mid-length of tube for a time period up to 700 μs. The results of FE analyses are compared with M-H shell theory and are presented in the next section.

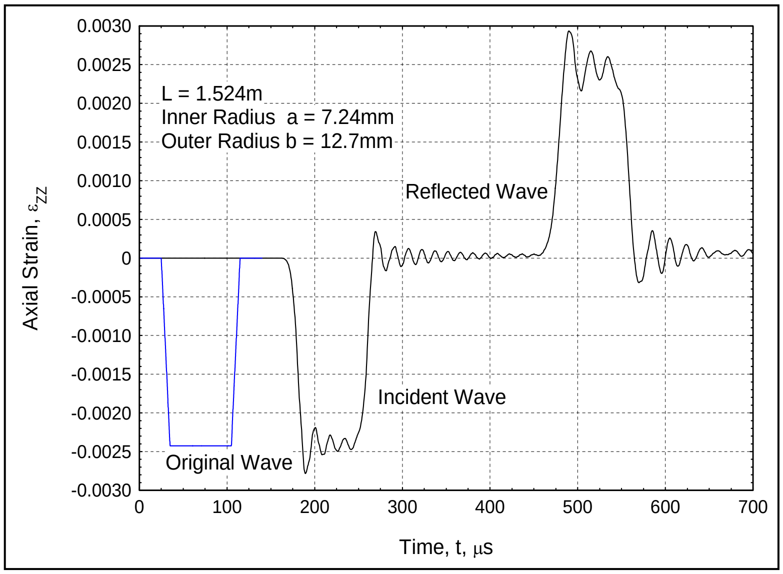

Figure 8. Strain vs. time at the mid-length of the tube.

5. Results and Discussion

The axial strain predictions by both M-H model and FE analysis for the two cylindrical tubes at z / L = 0.50–0.75 are presented in figures 9 and 10. When the M-H model is used, an implicit assumption is made that the wave propagation in the tubes is 1-D, and strain is determined from stress by Hooke's law $\varepsilon_{zz} = \sigma_{zz} / E$. Plots in the left column show the complete strain history, and the closer views in the peak region are listed in the right column. From the four plots in figures 9 and 10, it is obvious that the predictions by the M-H model and FEM analysis are very close. The rising parts of the waves are almost overlapping. For the peak part, the Pochhammer modes match very well. The only difference is that for the M-H model, the beginning part of the waves is abnormal, which will be explained later. The results in figures 9 and 10 prove that the cylindrical tubes in the SHPB experiment also vibrate in the first mode.

Figure 11 compares the wave dispersion results by the traditional algorithm, and the new algorithm used in this study. Here the strain data are plotted in the opposite sign. The results by the traditional algorithm are not smooth, and discontinuities are seen over the peak part of the waves. On the contrary, the modified algorithm predicts fairly smooth waveform. From the smooth waves, the number of Pochhammer modes can be clearly counted. If the old algorithm is compared to FE results, it is nearly impossible to reach the conclusion that wave motion in tubes follows the first-mode solution of M-H model. The comparison clearly verifies the correctness and necessity of the new algorithm.

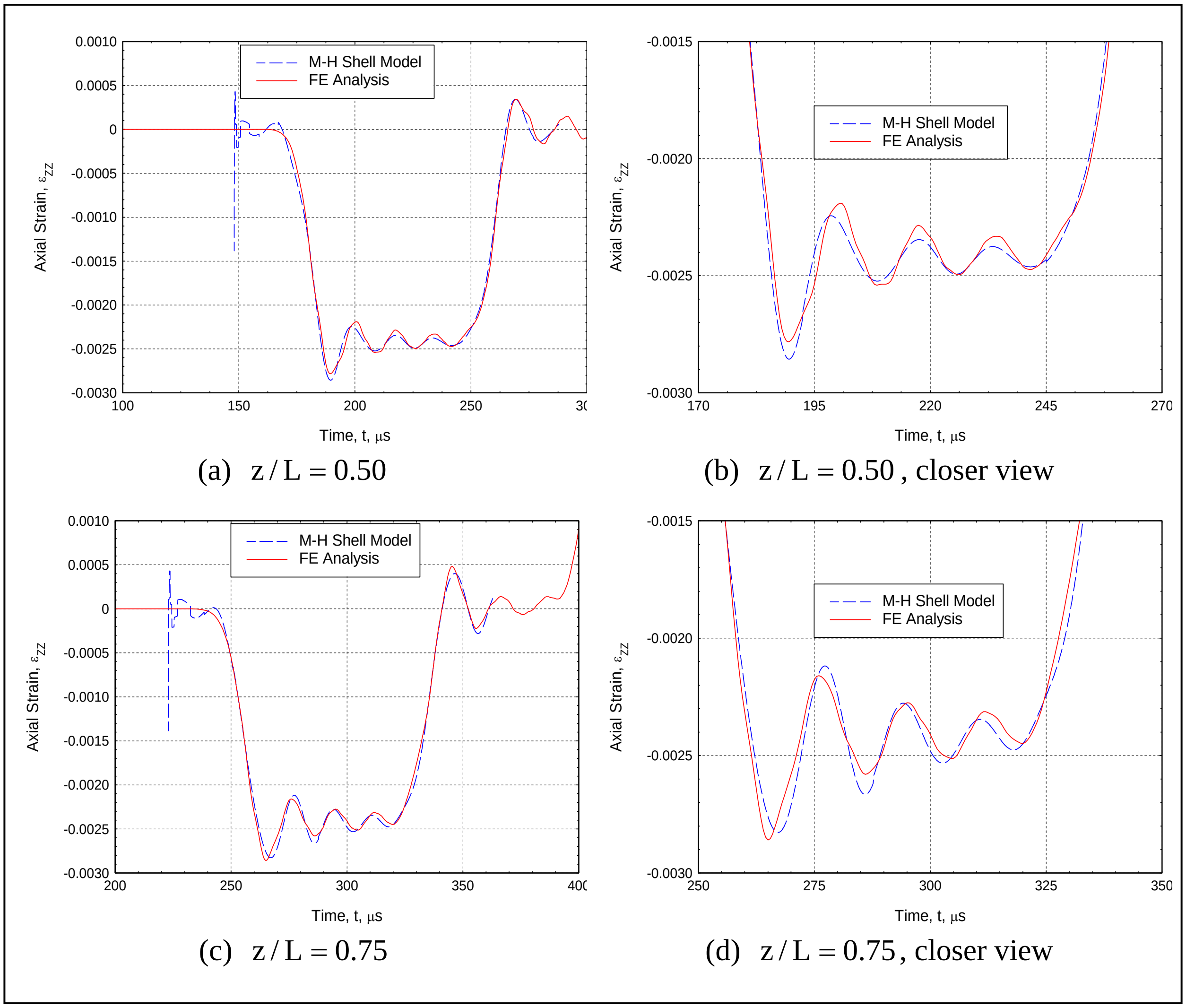

Figure 9. Axial strain predicted by M-H model and FE analysis for the tube with m = 0.548.

But why does the traditional algorithm work for rods? Figure 12 gives an example for the use of both algorithms on the rod with $\nu = 0.29$. It is seen that the predicted wave by traditional algorithm still has some discontinuous response in the later part of the wave peak, although the difference between the two algorithms is not as significant as for the tubes. From figure 3, it can be seen that the phase speed in rods changes very slowly with δ, compared with phase speed in tubes. This leads to more Pochhammer modes for rods than the tubes. Because the irregularities occur at the later part of the wave peak, the traditional algorithm still gives wave dispersion prediction accurate enough for engineering application, and the shortcoming of the traditional algorithm is concealed. In this study of wave dispersion in tubes, the limitation of the traditional wave dispersion algorithm is identified first.

The first part of the wave dispersion prediction by the new algorithm shows abnormal behavior. This is because at the beginning, relatively few wave components contribute to the dispersed wave, which can be seen from the algorithm described earlier. The M-H model assumes infinite

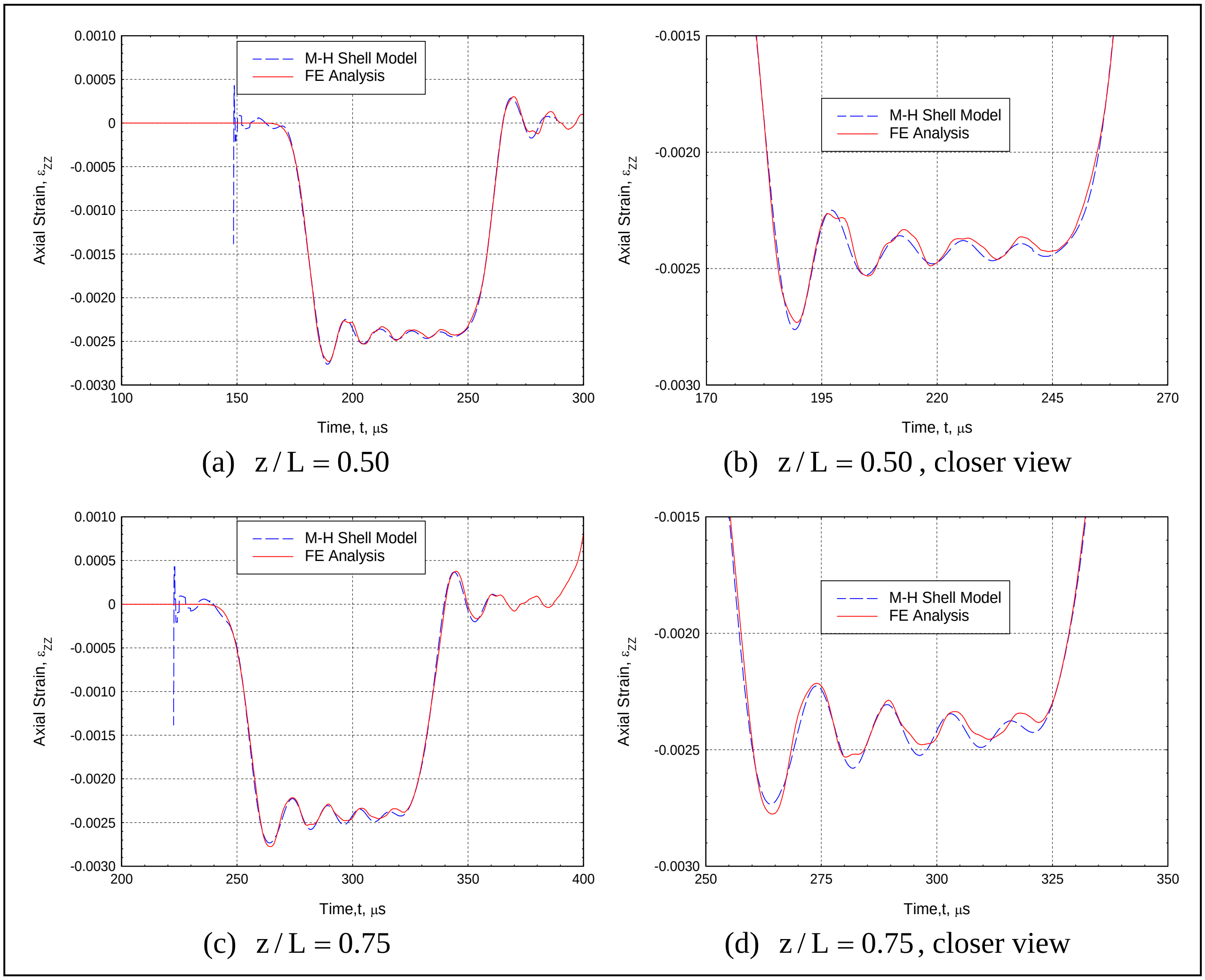

Figure 10. Axial strain predicted by M-H model and FE analysis for the tube with *m* = 0.667.

long tubes and continuous wave components. Under these assumptions, at any instance, all the wave components contribute to the whole waveform, so this abnormal behavior will not be seen. This phenomenon cannot be seen in real tests or in an FEM simulation either. When the new algorithm is used to predict the dispersed wave, it is assumed that the wave has period of 1400 μs during which the FT is performed. This input wave is a pulse wave rather than a continuous wave. The new algorithm does not allow any summation of wave components if the travel time condition is not satisfied. Thus the initial data are spurious till all the wave components have arrived at the particular point of interest. This problem can be resolved by taking a wider time window during FT and reducing the window during reconstruction.

When rods are used in the SHPB test, the only geometric parameter affecting the wave propagation in rods is the radius. If tubes are used in the SHPB test, two more parameters are involved: the inner radius and the *m* value. Among the outer radius, inner radius, tube wall

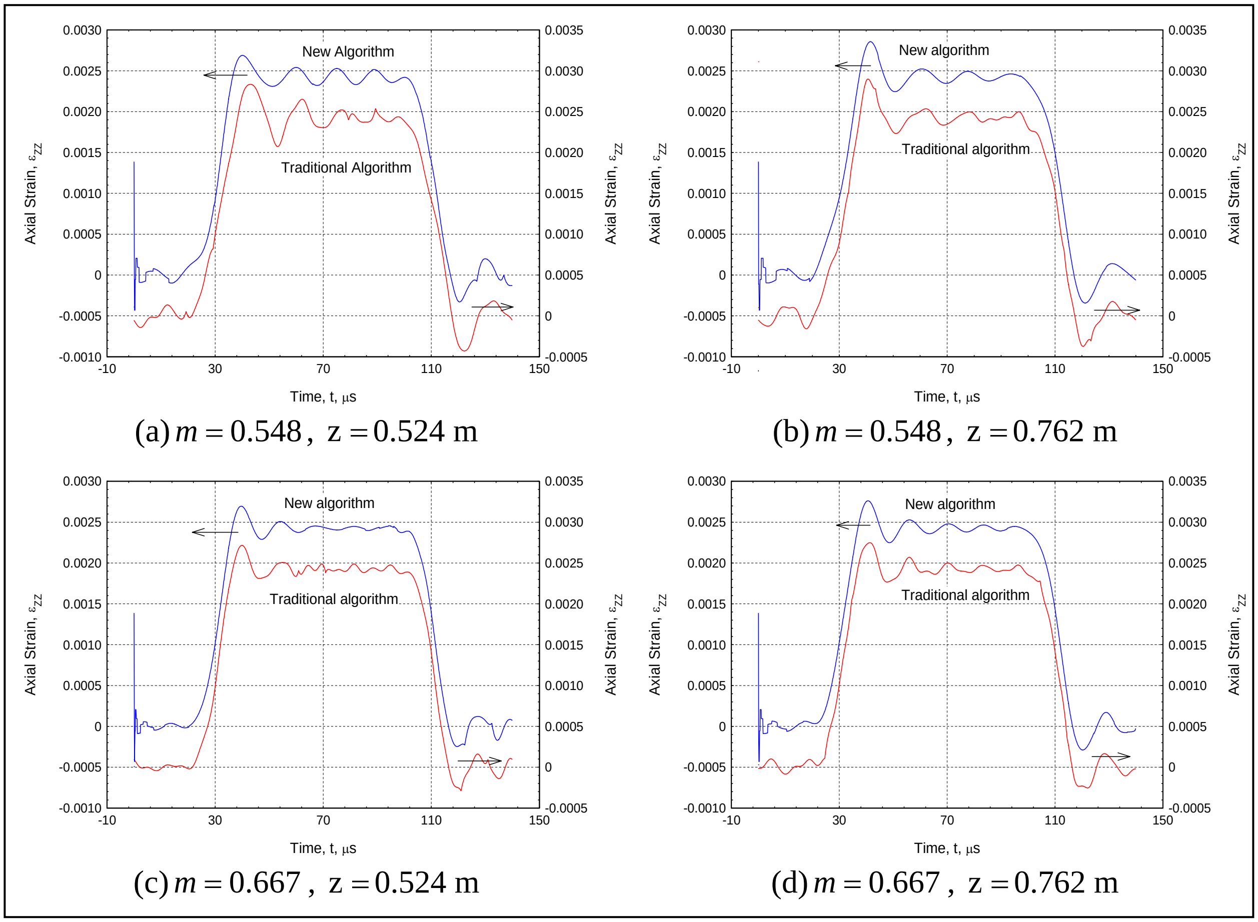

Figure 11. Comparison of new and traditional dispersion algorithms.

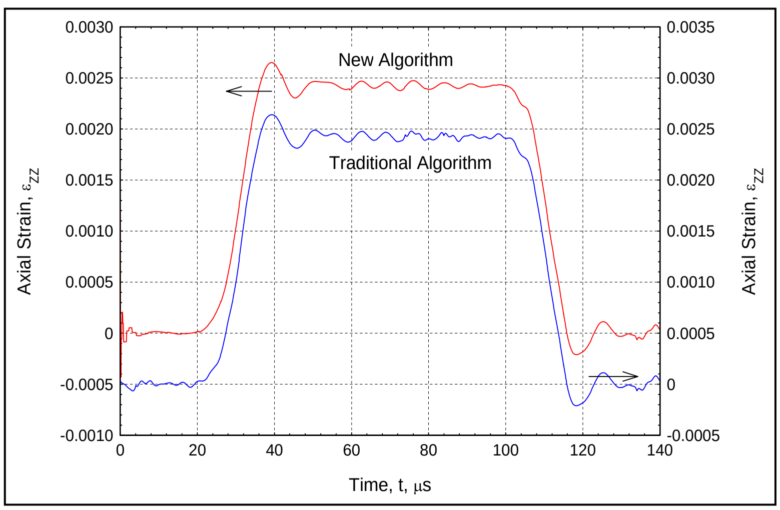

Figure 12. Dispersed wave in rod determined by the new algorithm and traditional algorithm. Material Poisson's ratio = 0.29.

thickness *h* and *m*, only two are independent. The discussion below will focus on *h* and *m*. It can be seen from figure 3 that when m takes lower values, the phase speed decreases more quickly when δ is small. For a fixed m value, when the tube wall is thinner, the phase speed for all the wave components will be closer than when the *h* value is higher. This can be seen graphically from figure 3. So lower m values and higher *h* values will make the phase speed decreases faster as a function of frequency, which will make the wave become wider and wider when it propagates in the tube. To catch all the wave components, a wider time window must be used to process the strain data. Usually a computer code is used to automatically select the processing window. For example, Leber's method (*18*) finds the processing window in the following way: first find a window between the point where the wave rises and the point where the wave drops to zero again. Another window that is ~33% wider than the first window and includes the first window in the middle is used as the processing window. If the wave becomes too wide, an incorrect window may be chosen which omits some important components. Furthermore, the incident wave, and the reflected wave will not contain the same amount of information because the reflected wave is wider than the incident wave, but the processing windows are still the same width. To obtain an accurate result, it is recommended to use a tube with higher m value and lower *h* value. Such a combination is actually not difficult to realize.

When tubes are used in the SHPB technique, several configurations of the apparatus are possible. If an incident tube and a transmission tube are used as the apparatus, it is recommended that one hollow cylindrical specimen be used. This requires that the tubes and the specimen have the same inner and outer diameters. The advantage of this configuration is that the 1-D requirement of the SHPB technique can be better satisfied than using rods. Figure 13 shows the stress history at the integration point of all the five elements at $z = 1.00$ m along the radial direction. It is seen that for all five elements, the axial stress history σ_{zz} vs. time is nearly the same. The normal stresses in the other two directions are also plotted. Figure 13 also shows that the stress σ_{xx} is very low (maximum is 13 MPa) compared to σ_{zz} (maximum is 580 MPa), and the stress σ_{yy} is even lower (maximum is 0.7 MPa). So the stress distribution can be considered as 1-D, and the axial stress distribution is uniform across the cross-section of the tube. The strains in x and y directions can be considered only due to Poisson's effect. Another option is described by Chen (*12*), where only the TT is used. When this configuration is used, a cap must be inserted between specimen and TT to transfer the load. It is not clear what effect this cap might have on the stress wave propagation and will be addressed in a separate work.

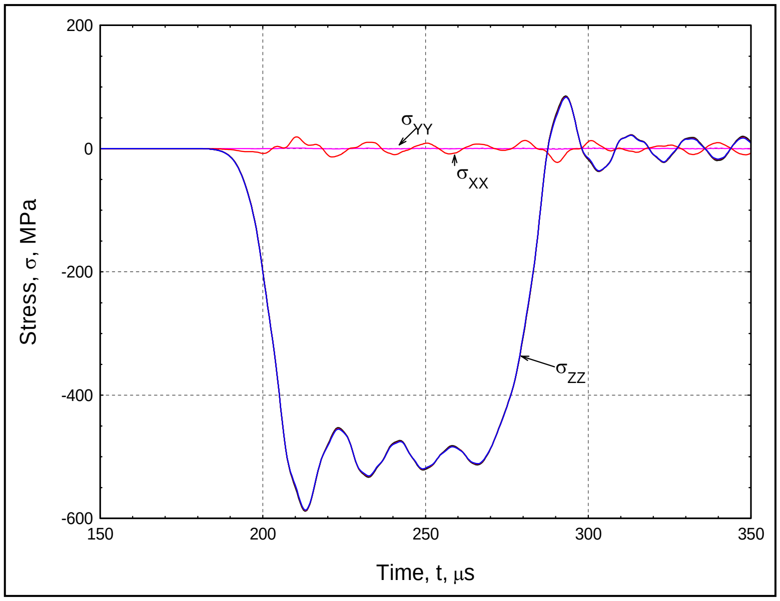

Figure 13. Stress history of all elements at z = 1.00 m along X = 0 axis.

6. Conclusions

In this report, wave dispersion in cylindrical tubes applied to the SHPB experiments is studied. The main conclusions are as follows:

1. The M-H shell model gives the same result as the 3-D model.
2. The FE study shows that wave propagation in tubes follows the first-mode solution of the M-H shell model.
3. A new dispersion algorithm is suggested, and it can better predict the dispersion wave.
4. For purpose of the SHPB application, tubes with higher *m* and lower *h* values should be used.

7. References

1. Hopkinson, B. A Method of Measuring the Pressure in the Deformation of High Explosives by the Impact of Bullets. *Philosophical Transactions of the Royal Society of London* **1914**, *A213*, 437–452.

2. Davies, R. M. A Critical Study of the Hopkinson Pressure Bar. *Philosophical Transactions of the Royal Society of London, Series A, Mathematical and Physical Sciences* **1948**, *240*, 375–457.

3. Kolsky, H. An Investigation of the Mechanical Properties of Materials at Very High Rates of Loading. *Proceedings of the Royal Society of London* 1949, *B62*, 676–700.

4. Pochhammer, L. Uber die Fortpflanzungsgeschwindigkeiten kleiner Schwing ungen in einem unbegrenzten isotropen Kreiscylinder. *Journal fur Mathematick (Crelle)* **1876**, *81*, 324–336.

5. Chree, C. The Equations of an Isotropic Elastic Solid in Polar and Cylindrical Co-ords. Their Solutions and Applications. *Cambridge Philosophical Society: Transactions* **1889**, *14*, 250–369.

6. Bancroft, D. The Speed of Longitudinal Waves in Cylindrical Bars. *Physical Review* **1941**, *59*, 588–593.

7. Follansbee, P. S.; Frantz C. Wave Propagation in the Split Hopkinson Pressure Bar. *Journal of Engineering Materials and Technology* **1983**, *105*, 61–66.

8. Gong, J. C.; Malvern, L. E.; Jenkins, D. A. Dispersion Investigation in the Split Hopkinson Pressure Bar. *Journal of Engineering Materials and Technology* **1990**, *112*, 309–314.

9. Li, Z. H.; Lambros, J. Determination of the Dynamic Response of Brittle Composites by the Use of the Split Hopkinson Pressure Bar. *Composite Science and Technology* **1999**, *59*, 1097–1107.

10. Dowling, A. R.; Harding, J.; Campell, J. D. The Dynamic Punching of Metals. *Journal of the Institute of Metals* **1970**, *98*, 215–224.

11. Zhao, H.; Gary, G.; Klepaczko, J. R. On the Use of a Visco-Elastic Split Hopkinson Pressure Bar. *International Journal of Impact Engineering* **1997**, *19*, 319–330.

12. Chen, W.; Zhang, B.; Forrestal, M. J. A Split Hopkinson Bar Technique for Low-Impedance Materials. *Experimental Mechanics* **1999**, *39*, 81–85.

13. Ghosh, J. Longitudinal Vibrations of a Hollow Cylinder. *Bulletin Calcutta Mathematical Society* **1923**, *14*, 31–40.

14. Fay, R. D. Waves in Liquid-Filled Cylinders. *The Journal of Acoustical Society of America* **1952**, *24*, 459–462.

15. Herrmann, G.; Mirsky, I. Three-Dimensional and Shell-Theory Analysis of Axially Symmetric Motions of Cylinders. *Journal of Applied Mechanics* **1956**, *23*, 563–568.

16. Mirsky, I.; Herrmann, G. Axially Symmetric Motions of Thick Cylindrical Shells. *Journal of Applied Mechanics* **1958**, *25*, 97–102.

17. Felice, C. W. *The Response of Soil to Impulse Loads Using the Split Hopkinson Pressure Bar Technique*; AFWL-TR-8-92; Air Force Weapons Laboratory: Kirtland Air Force Base, NM, May 1986.

18. Lifshitz, J. M.; Leber, H. Data Processing in the Split Hopkinson Pressure Bar Tests. *International Journal of Impact Engineering* **1994**, *15* (6), 723–733.

NO. OF COPIES	ORGANIZATION
1 (PDF ONLY)	DEFENSE TECHNICAL INFORMATION CTR DTIC OCA 8725 JOHN J KINGMAN RD STE 0944 FT BELVOIR VA 22060-6218
1	COMMANDING GENERAL US ARMY MATERIEL CMD AMCRDA TF 5001 EISENHOWER AVE ALEXANDRIA VA 22333-0001
1	INST FOR ADVNCD TCHNLGY THE UNIV OF TEXAS AT AUSTIN 3925 W BRAKER LN STE 400 AUSTIN TX 78759-5316
1	US MILITARY ACADEMY MATH SCI CTR EXCELLENCE MADN MATH THAYER HALL WEST POINT NY 10996-1786
1	DIRECTOR US ARMY RESEARCH LAB IMNE AD IM DR 2800 POWDER MILL RD ADELPHI MD 20783-1197
3	DIRECTOR US ARMY RESEARCH LAB AMSRD ARL CI OK TL 2800 POWDER MILL RD ADELPHI MD 20783-1197
3	DIRECTOR US ARMY RESEARCH LAB AMSRD ARL CS IS T 2800 POWDER MILL RD ADELPHI MD 20783-1197

NO. OF COPIES	ORGANIZATION
	ABERDEEN PROVING GROUND
1	DIR USARL AMSRD ARL CI OK TP (BLDG 4600)

NO. OF COPIES	ORGANIZATION
1	DIRECTOR US ARMY RESEARCH LAB AMSRD ARL SE L D SNIDER 2800 POWDER MILL RD ADELPHI MD 20783-1197
1	DIRECTOR US ARMY RESEARCH LAB AMSRD ARL SE DE R ATKINSON 2800 POWDER MILL RD ADELPHI MD 20783-1197
5	DIRECTOR US ARMY RESEARCH LAB AMSRD ARL WM MB A ABRAHAMIAN M BERMAN M CHOWDHURY T LI E SZYMANSKI 2800 POWDER MILL RD ADELPHI MD 20783-1197
1	COMMANDER US ARMY MATERIEL CMD AMXMI INT 5001 EISENHOWER AVE ALEXANDRIA VA 22333-0001
2	PM MAS SFAE AMO MAS MC PICATINNY ARSENAL NJ 07806-5000
3	COMMANDER US ARMY ARDEC AMSTA AR CC M PADGETT J HEDDERICH H OPAT PICATINNY ARSENAL NJ 07806-5000
2	COMMANDER US ARMY ARDEC AMSTA AR AE WW E BAKER J PEARSON PICATINNY ARSENAL NJ 07806-5000

NO. OF COPIES	ORGANIZATION
1	COMMANDER US ARMY ARDEC AMSTA AR FSE PICATINNY ARSENAL NJ 07806-5000
1	COMMANDER US ARMY ARDEC AMSTA AR TD PICATINNY ARSENAL NJ 07806-5000
13	COMMANDER US ARMY ARDEC AMSTA AR CCH A F ALTAMURA M NICOLICH M PALATHINGUL D VO R HOWELL A VELLA M YOUNG L MANOLE S MUSALLI R CARR M LUCIANO E LOGSDEN T LOUZEIRO PICATINNY ARSENAL NJ 07806-5000
1	COMMANDER US ARMY ARDEC AMSTA AR CCH P J LUTZ PICATINNY ARSENAL NJ 07806-5000
1	COMMANDER US ARMY ARDEC AMSTA AR FSF T C LIVECCHIA PICATINNY ARSENAL NJ 07806-5000
1	COMMANDER US ARMY ARDEC AMSTA ASF PICATINNY ARSENAL NJ 07806-5000

NO. OF
COPIES ORGANIZATION

1 COMMANDER
US ARMY ARDEC
AMSTA AR QAC T C
J PAGE
PICATINNY ARSENAL NJ
07806-5000

1 COMMANDER
US ARMY ARDEC
AMSTA AR M
D DEMELLA
PICATINNY ARSENAL NJ
07806-5000

3 COMMANDER
US ARMY ARDEC
AMSTA AR FSA
A WARNASH
B MACHAK
M CHIEFA
PICATINNY ARSENAL NJ
07806-5000

2 COMMANDER
US ARMY ARDEC
AMSTA AR FSP G
M SCHIKSNIS
D CARLUCCI
PICATINNY ARSENAL NJ
07806-5000

2 COMMANDER
US ARMY ARDEC
AMSTA AR CCH C
H CHANIN
S CHICO
PICATINNY ARSENAL NJ
07806-5000

1 COMMANDER
US ARMY ARDEC
AMSTA AR QAC T
D RIGOGLIOSO
PICATINNY ARSENAL NJ
07806-5000

1 COMMANDER
US ARMY ARDEC
AMSTA AR WET
T SACHAR
BLDG 172
PICATINNY ARSENAL NJ
07806-5000

NO. OF
COPIES ORGANIZATION

1 US ARMY ARDEC
INTELLIGENCE SPECIALIST
AMSTA AR WEL F
M GUERRIERE
PICATINNY ARSENAL NJ
07806-5000

10 COMMANDER
US ARMY ARDEC
AMSTA AR CCH B
P DONADIA
F DONLON
P VALENTI
C KNUTSON
G EUSTICE
K HENRY
J MCNABOC
G WAGNECZ
R SAYER
F CHANG
PICATINNY ARSENAL NJ
07806-5000

6 COMMANDER
US ARMY ARDEC
AMSTA AR CCL
F PUZYCKI
R MCHUGH
D CONWAY
E JAROSZEWSKI
R SCHLENNER
M CLUNE
PICATINNY ARSENAL NJ
07806-5000

1 PM ARMS
SFAE GCSS ARMS
BLDG 171
PICATINNY ARSENAL NJ
07806-5000

1 COMMANDER
US ARMY ARDEC
AMSTA AR WEA
J BRESCIA
PICATINNY ARSENAL NJ
07806-5000

1 PM MAS
SFAE AMO MAS
PICATINNY ARSENAL NJ
07806-5000

NO. OF COPIES	ORGANIZATION
1	PM MAS SFAE AMO MAS CHIEF ENGINEER PICATINNY ARSENAL NJ 07806-5000
1	PM MAS SFAE AMO MAS PS PICATINNY ARSENAL NJ 07806-5000
2	PM MAS SFAE AMO MAS LC PICATINNY ARSENAL NJ 07806-5000
1	COMMANDER US ARMY ARDEC PRODUCTION BASE MODERN ACTY AMSMC PBM K PICATINNY ARSENAL NJ 07806-5000
1	COMMANDER US ARMY TACOM PM COMBAT SYSTEMS SFAE GCS CS 6501 ELEVEN MILE RD WARREN MI 48397-5000
1	COMMANDER US ARMY TACOM AMSTA SF WARREN MI 48397-5000
1	DIRECTOR AIR FORCE RESEARCH LAB MLLMD D MIRACLE 2230 TENTH ST WRIGHT PATTERSON AFB OH 45433-7817
1	OFC OF NAVAL RESEARCH J CHRISTODOULOU ONR CODE 332 800 N QUINCY ST ARLINGTON VA 22217-5600
1	US ARMY CERL R LAMPO 2902 NEWMARK DR CHAMPAIGN IL 61822

NO. OF COPIES	ORGANIZATION
1	COMMANDER US ARMY TACOM PM SURVIVABLE SYSTEMS SFAE GCSS W GSI H M RYZYI 6501 ELEVEN MILE RD WARREN MI 48397-5000
1	COMMANDER US ARMY TACOM CHIEF ABRAMS TESTING SFAE GCSS W AB QT T KRASKIEWICZ 6501 ELEVEN MILE RD WARREN MI 48397-5000
1	COMMANDER WATERVLIET ARSENAL SMCWV QAE Q B VANINA BLDG 44 WATERVLIET NY 12189-4050
1	TNG, DOC, & CBT DEV ATZK TDD IRSA A POMEY FT KNOX KY 40121
2	HQ IOC TANK AMMUNITION TEAM AMSIO SMT R CRAWFORD W HARRIS ROCK ISLAND IL 61299-6000
2	COMMANDER US ARMY AMCOM AVIATION APPLIED TECH DIR J SCHUCK FT EUSTIS VA 23604-5577
1	NSWC DAHLGREN DIV CODE G06 DAHLGREN VA 22448
2	US ARMY CORPS OF ENGR CERD C T LIU CEW ET T TAN 20 MASSACHUSETTS AVE NW WASHINGTON DC 20314

NO. OF COPIES	ORGANIZATION
1	US ARMY COLD REGIONS RSCH & ENGRNG LAB P DUTTA 72 LYME RD HANOVER NH 03755
14	COMMANDER US ARMY TACOM AMSTA TR R R MCCLELLAND D THOMAS J BENNETT D HANSEN AMSTA JSK S GOODMAN J FLORENCE K IYER D TEMPLETON A SCHUMACHER AMSTA TR D D OSTBERG L HINOJOSA B RAJU AMSTA CS SF H HUTCHINSON F SCHWARZ WARREN MI 48397-5000
14	BENET LABS AMSTA AR CCB R FISCELLA M SOJA E KATHE M SCAVULO G SPENCER P WHEELER S KRUPSKI J VASILAKIS G FRIAR R HASENBEIN AMSTA CCB R S SOPOK E HYLAND D CRAYON R DILLON WATERVLIET NY 12189-4050
1	USA SBCCOM PM SOLDIER SPT AMSSB PM RSS A J CONNORS KANSAS ST NATICK MA 01760-5057

NO. OF COPIES	ORGANIZATION
1	NSWC TECH LIBRARY CODE 323 17320 DAHLGREN RD DAHLGREN VA 22448
2	USA SBCCOM MATERIAL SCIENCE TEAM AMSSB RSS J HERBERT M SENNETT KANSAS ST NATICK MA 01760-5057
2	OFC OF NAVAL RESEARCH D SIEGEL CODE 351 J KELLY 800 N QUINCY ST ARLINGTON VA 22217-5660
1	NSWC CRANE DIVISION M JOHNSON CODE 20H4 LOUISVILLE KY 40214-5245
2	NSWC U SORATHIA C WILLIAMS CD 6551 9500 MACARTHUR BLVD WEST BETHESDA MD 20817
2	COMMANDER NSWC CARDEROCK DIVISION R PETERSON CODE 2020 M CRITCHFIELD CODE 1730 BETHESDA MD 20084
8	DIRECTOR US ARMY NGIC D LEITER MS 404 M HOLTUS MS 301 M WOLFE MS 307 S MINGLEDORF MS 504 J GASTON MS 301 W GSTATTENBAUER MS 304 R WARNER MS 305 J CRIDER MS 306 2055 BOULDERS RD CHARLOTTESVILLE VA 22911-8318

NO. OF COPIES	ORGANIZATION
1	NAVAL SEA SYSTEMS CMD D LIESE 1333 ISAAC HULL AVE SE 1100 WASHINGTON DC 20376-1100
1	EXPEDITIONARY WARFARE DIV N85 F SHOUP 2000 NAVY PENTAGON WASHINGTON DC 20350-2000
8	US ARMY SBCCOM SOLDIER SYSTEMS CENTER BALLISTICS TEAM J WARD W ZUKAS P CUNNIFF J SONG MARINE CORPS TEAM J MACKIEWICZ BUS AREA ADVOCACY TEAM W HASKELL AMSSB RCP SS W NYKVIST S BEAUDOIN KANSAS ST NATICK MA 01760-5019
7	US ARMY RESEARCH OFC A CROWSON H EVERETT J PRATER G ANDERSON D STEPP D KISEROW J CHANG PO BOX 12211 RESEARCH TRIANGLE PARK NC 27709-2211
1	AFRL MLBC 2941 P ST RM 136 WRIGHT PATTERSON AFB OH 45433-7750
1	DIRECTOR LOS ALAMOS NATL LAB F L ADDESSIO T 3 MS 5000 PO BOX 1633 LOS ALAMOS NM 87545

NO. OF COPIES	ORGANIZATION
8	NSWC J FRANCIS CODE G30 D WILSON CODE G32 R D COOPER CODE G32 J FRAYSSE CODE G33 E ROWE CODE G33 T DURAN CODE G33 L DE SIMONE CODE G33 R HUBBARD CODE G33 DAHLGREN VA 22448
1	NSWC CARDEROCK DIVISION R CRANE CODE 6553 9500 MACARTHUR BLVD WEST BETHESDA MD 20817-5700
1	AFRL MLSS R THOMSON 2179 12TH ST RM 122 WRIGHT PATTERSON AFB OH 45433-7718
2	AFRL F ABRAMS J BROWN BLDG 653 2977 P ST STE 6 WRIGHT PATTERSON AFB OH 45433-7739
5	DIRECTOR LLNL R CHRISTENSEN S DETERESA F MAGNESS M FINGER MS 313 M MURPHY L 282 PO BOX 808 LIVERMORE CA 94550
1	AFRL MLS OL L COULTER 5851 F AVE BLDG 849 RM AD1A HILL AFB UT 84056-5713
1	OSD JOINT CCD TEST FORCE OSD JCCD R WILLIAMS 3909 HALLS FERRY RD VICKSBURG MS 29180-6199

NO. OF COPIES	ORGANIZATION
3	DARPA M VANFOSSEN S WAX L CHRISTODOULOU 3701 N FAIRFAX DR ARLINGTON VA 22203-1714
2	SERDP PROGRAM OFC PM P2 C PELLERIN B SMITH 901 N STUART ST STE 303 ARLINGTON VA 22203
1	OAK RIDGE NATL LAB R M DAVIS PO BOX 2008 OAK RIDGE TN 37831-6195
1	OAK RIDGE NATL LAB C EBERLE MS 8048 PO BOX 2008 OAK RIDGE TN 37831
3	DIRECTOR SANDIA NATL LABS APPLIED MECHS DEPT MS 9042 J HANDROCK Y R KAN J LAUFFER PO BOX 969 LIVERMORE CA 94551-0969
1	OAK RIDGE NATL LAB C D WARREN MS 8039 PO BOX 2008 OAK RIDGE TN 37831
4	NIST M VANLANDINGHAM MS 8621 J CHIN MS 8621 J MARTIN MS 8621 D DUTHINH MS 8611 100 BUREAU DR GAITHERSBURG MD 20899
1	HYDROGEOLOGIC INC SERDP ESTCP SPT OFC S WALSH 1155 HERNDON PKWY STE 900 HERNDON VA 20170

NO. OF COPIES	ORGANIZATION
3	NASA LANGLEY RESEARCH CTR AMSRD ARL VS W ELBER MS 266 F BARTLETT JR MS 266 G FARLEY MS 266 HAMPTON VA 23681-0001
1	NASA LANGLEY RESEARCH CTR T GATES MS 188E HAMPTON VA 23661-3400
1	FHWA E MUNLEY 6300 GEORGETOWN PIKE MCLEAN VA 22101
1	USDOT FEDERAL RAILROAD M FATEH RDV 31 WASHINGTON DC 20590
3	CYTEC FIBERITE R DUNNE D KOHLI R MAYHEW 1300 REVOLUTION ST HAVRE DE GRACE MD 21078
1	DIRECTOR NGIC IANG TMT 2055 BOULDERS RD CHARLOTTESVILLE VA 22911-8318
1	SIOUX MFG B KRIEL PO BOX 400 FT TOTTEN ND 58335
2	3TEX CORP A BOGDANOVICH J SINGLETARY 109 MACKENAN DR CARY NC 27511
1	3M CORP J SKILDUM 3M CENTER BLDG 60 IN 01 ST PAUL MN 55144-1000

NO. OF COPIES	ORGANIZATION
1	DIRECTOR DEFENSE INTLLGNC AGNCY TA 5 K CRELLING WASHINGTON DC 20310
1	ADVANCED GLASS FIBER YARNS T COLLINS 281 SPRING RUN LANE STE A DOWNINGTON PA 19335
1	COMPOSITE MATERIALS INC D SHORTT 19105 63 AVE NE PO BOX 25 ARLINGTON WA 98223
1	JPS GLASS L CARTER PO BOX 260 SLATER RD SLATER SC 29683
1	COMPOSITE MATERIALS INC R HOLLAND 11 JEWEL CT ORINDA CA 94563
1	COMPOSITE MATERIALS INC C RILEY 14530 S ANSON AVE SANTA FE SPRINGS CA 90670
2	SIMULA J COLTMAN R HUYETT 10016 S 51ST ST PHOENIX AZ 85044
2	PROTECTION MATERIALS INC M MILLER F CRILLEY 14000 NW 58 CT MIAMI LAKES FL 33014
2	FOSTER MILLER M ROYLANCE W ZUKAS 195 BEAR HILL RD WALTHAM MA 02354-1196

NO. OF COPIES	ORGANIZATION
1	ROM DEVELOPMENT CORP R O MEARA 136 SWINEBURNE ROW BRICK MARKET PLACE NEWPORT RI 02840
2	TEXTRON SYSTEMS T FOLTZ M TREASURE 1449 MIDDLESEX ST LOWELL MA 01851
1	O GARA HESS & EISENHARDT M GILLESPIE 9113 LESAINT DR FAIRFIELD OH 45014
2	MILLIKEN RESEARCH CORP H KUHN M MACLEOD PO BOX 1926 SPARTANBURG SC 29303
1	CONNEAUGHT INDUSTRIES INC J SANTOS PO BOX 1425 COVENTRY RI 02816
1	ARMTEC DEFENSE PRODUCTS S DYER 85 901 AVE 53 PO BOX 848 COACHELLA CA 92236
1	NATL COMPOSITE CTR T CORDELL 2000 COMPOSITE DR KETTERING OH 45420
3	PACIFIC NORTHWEST LAB M SMITH G VAN ARSDALE R SHIPPELL PO BOX 999 RICHLAND WA 99352
1	SAIC M PALMER 1410 SPRING HILL RD STE 400 MS SH4 5 MCLEAN VA 22102

NO. OF COPIES	ORGANIZATION
1	ALLIANT TECHSYSTEMS INC 4700 NATHAN LN N PLYMOUTH MN 55442-2512
1	APPLIED COMPOSITES W GRISCH 333 NORTH SIXTH ST ST CHARLES IL 60174
1	CUSTOM ANALYTICAL ENG SYS INC A ALEXANDER 13000 TENSOR LANE NE FLINTSTONE MD 21530
1	AAI CORP DR N B MCNELLIS PO BOX 126 HUNT VALLEY MD 21030-0126
1	OFC DEPUTY UNDER SEC DEFNS J THOMPSON 1745 JEFFERSON DAVIS HWY CRYSTAL SQ 4 STE 501 ARLINGTON VA 22202
3	ALLIANT TECHSYSTEMS INC J CONDON E LYNAM J GERHARD WV01 16 STATE RT 956 PO BOX 210 ROCKET CENTER WV 26726-0210
1	PROJECTILE TECHNOLOGY INC 515 GILES ST HAVRE DE GRACE MD 21078
1	HEXCEL INC R BOE PO BOX 18748 SALT LAKE CITY UT 84118
1	PRATT & WHITNEY C WATSON 400 MAIN ST MS 114 37 EAST HARTFORD CT 06108

NO. OF COPIES	ORGANIZATION
5	NORTHROP GRUMMAN B IRWIN K EVANS D EWART A SHREKENHAMER J MCGLYNN BLDG 160 DEPT 3700 1100 WEST HOLLYVALE ST AZUSA CA 91701
1	HERCULES INC HERCULES PLAZA WILMINGTON DE 19894
1	BRIGS COMPANY J BACKOFEN 2668 PETERBOROUGH ST HERNDON VA 22071-2443
1	ZERNOW TECHNICAL SERVICES L ZERNOW 425 W BONITA AVE STE 208 SAN DIMAS CA 91773
1	GENERAL DYNAMICS OTS L WHITMORE 10101 NINTH ST NORTH ST PETERSBURG FL 33702
2	GENERAL DYNAMICS OTS FLINCHBAUGH DIV K LINDE T LYNCH PO BOX 127 RED LION PA 17356
1	GKN WESTLAND AEROSPACE D OLDS 450 MURDOCK AVE MERIDEN CT 06450-8324
2	BOEING ROTORCRAFT P MINGURT P HANDEL 800 B PUTNAM BLVD WALLINGFORD PA 19086

NO. OF COPIES	ORGANIZATION
5	SIKORSKY AIRCRAFT G JACARUSO T CARSTENSAN B KAY S GARBO MS S330A J ADELMANN 6900 MAIN ST PO BOX 9729 STRATFORD CT 06497-9729
1	AEROSPACE CORP G HAWKINS M4 945 2350 E EL SEGUNDO BLVD EL SEGUNDO CA 90245
2	CYTEC FIBERITE M LIN W WEB 1440 N KRAEMER BLVD ANAHEIM CA 92806
2	UDLP G THOMAS M MACLEAN PO BOX 58123 SANTA CLARA CA 95052
1	UDLP WARREN OFC A LEE 31201 CHICAGO RD SOUTH SUITE B102 WARREN MI 48093
2	UDLP R BRYNSVOLD P JANKE MS 170 4800 EAST RIVER RD MINNEAPOLIS MN 55421-1498
1	LOCKHEED MARTIN SKUNK WORKS D FORTNEY 1011 LOCKHEED WAY PALMDALE CA 93599-2502
1	LOCKHEED MARTIN R FIELDS 5537 PGA BLVD SUITE 4516 ORLANDO FL 32839

NO. OF COPIES	ORGANIZATION
1	NORTHRUP GRUMMAN CORP ELECTRONIC SENSORS & SYSTEMS DIV E SCHOCH MS V 16 1745A W NURSERY RD LINTHICUM MD 21090
1	GDLS DIVISION D BARTLE PO BOX 1901 WARREN MI 48090
2	GDLS D REES M PASIK PO BOX 2074 WARREN MI 48090-2074
1	GDLS MUSKEGON OPER M SOIMAR 76 GETTY ST MUSKEGON MI 49442
1	GENERAL DYNAMICS AMPHIBIOUS SYS SURVIVABILITY LEAD G WALKER 991 ANNAPOLIS WAY WOODBRIDGE VA 22191
6	INST FOR ADVANCED TECH H FAIR I MCNAB P SULLIVAN S BLESS W REINECKE C PERSAD 3925 W BRAKER LN STE 400 AUSTIN TX 78759-5316
1	ARROW TECH ASSOC 1233 SHELBURNE RD STE D8 SOUTH BURLINGTON VT 05403-7700
1	R EICHELBERGER CONSULTANT 409 W CATHERINE ST BEL AIR MD 21014-3613

NO. OF COPIES	ORGANIZATION
1	SAIC G CHRYSSOMALLIS 8500 NORMANDALE LAKE BLVD SUITE 1610 BLOOMINGTON MN 55437-3828
1	UCLA MANE DEPT ENGR IV H T HAHN LOS ANGELES CA 90024-1597
2	UNIV OF DAYTON RESEARCH INST R Y KIM A K ROY 300 COLLEGE PARK AVE DAYTON OH 45469-0168
1	UMASS LOWELL PLASTICS DEPT N SCHOTT 1 UNIVERSITY AVE LOWELL MA 01854
1	IIT RESEARCH CTR D ROSE 201 MILL ST ROME NY 13440-6916
1	GA TECH RESEARCH INST GA INST OF TCHNLGY P FRIEDERICH ATLANTA GA 30392
1	MICHIGAN ST UNIV MSM DEPT R AVERILL 3515 EB EAST LANSING MI 48824-1226
1	UNIV OF WYOMING D ADAMS PO BOX 3295 LARAMIE WY 82071
1	PENN STATE UNIV R S ENGEL 245 HAMMOND BLDG UNIVERSITY PARK PA 16801

NO. OF COPIES	ORGANIZATION
2	PENN STATE UNIV R MCNITT C BAKIS 212 EARTH ENGR SCIENCES BLDG UNIVERSITY PARK PA 16802
1	PURDUE UNIV SCHOOL OF AERO & ASTRO C T SUN W LAFAYETTE IN 47907-1282
1	STANFORD UNIV DEPT OF AERONAUTICS & AEROBALLISTICS S TSAI DURANT BLDG STANFORD CA 94305
1	UNIV OF MAINE ADV STR & COMP LAB R LOPEZ ANIDO 5793 AEWC BLDG ORONO ME 04469-5793
1	JOHNS HOPKINS UNIV APPLIED PHYSICS LAB P WIENHOLD 11100 JOHNS HOPKINS RD LAUREL MD 20723-6099
1	UNIV OF DAYTON J M WHITNEY COLLEGE PARK AVE DAYTON OH 45469-0240
1	NORTH CAROLINA ST UNIV CIVIL ENGINEERING DEPT W RASDORF PO BOX 7908 RALEIGH NC 27696-7908
5	UNIV OF DELAWARE CTR FOR COMPOSITE MTRLS J GILLESPIE M SANTARE S YARLAGADDA S ADVANI D HEIDER 201 SPENCER LAB NEWARK DE 19716

NO. OF COPIES	ORGANIZATION
1	DEPT OF MTRLS SCIENCE & ENGRG UNIV OF ILLINOIS AT URBANA CHAMPAIGN J ECONOMY 1304 WEST GREEN ST 115B URBANA IL 61801
1	UNIV OF MARYLAND DEPT OF AEROSPACE ENGRG A J VIZZINI COLLEGE PARK MD 20742
1	DREXEL UNIV A S D WANG 3141 CHESTNUT ST PHILADELPHIA PA 19104
3	UNIV OF TEXAS AT AUSTIN CTR FOR ELECTROMECHANICS J PRICE A WALLS J KITZMILLER 10100 BURNET RD AUSTIN TX 78758-4497
3	VA POLYTECHNICAL INST & STATE UNIV DEPT OF ESM M W HYER K REIFSNIDER R JONES BLACKSBURG VA 24061-0219
1	SOUTHWEST RESEARCH INST ENGR & MATL SCIENCES DIV J RIEGEL 6220 CULEBRA RD PO DRAWER 28510 SAN ANTONIO TX 78228-0510
1	BATELLE NATICK OPERS B HALPIN 313 SPEEN ST NATICK MA 01760
3	DIRECTOR US ARMY RESEARCH LAB AMSRD ARL WM MB A FRYDMAN 2800 POWDER MILL RD ADELPHI MD 20783-1197

NO. OF COPIES	ORGANIZATION
	ABERDEEN PROVING GROUND
1	US ARMY ATC CSTE DTC AT AC I W C FRAZER 400 COLLERAN RD APG MD 21005-5059
91	DIR USARL AMSRD ARL CI AMSRD ARL O AP EG M ADAMSON AMSRD ARL SL BA AMSRD ARL SL BB D BELY AMSRD ARL WM J SMITH H WALLACE AMSRD ARL WM B A HORST T KOGLER AMSRD ARL WM BA D LYON AMSRD ARL WM BC J NEWILL P PLOSTINS A ZIELINSKI AMSRD ARL WM BD P CONROY B FORCH M LEADORE C LEVERITT R LIEB R PESCE RODRIGUEZ B RICE AMSRD ARL WM BF S WILKERSON AMSRD ARL WM M B FINK J MCCAULEY AMSRD ARL WM MA L GHIORSE S MCKNIGHT E WETZEL AMSRD ARL WM MB J BENDER T BOGETTI L BURTON R CARTER K CHO W DE ROSSET G DEWING R DOWDING W DRYSDALE

NO. OF COPIES	ORGANIZATION
	R EMERSON D HENRY D HOPKINS R KASTE L KECSKES M MINNICINO B POWERS D SNOHA J SOUTH M STAKER J SWAB J TZENG AMSRD ARL WM MC J BEATTY R BOSSOLI E CHIN S CORNELISON D GRANVILLE B HART J LASALVIA J MONTGOMERY F PIERCE E RIGAS W SPURGEON AMSRD ARL WM MD B CHEESEMAN P DEHMER R DOOLEY G GAZONAS S GHIORSE C HOPPEL M KLUSEWITZ W ROY J SANDS D SPAGNUOLO S WALSH S WOLF AMSRD ARL WM RP J BORNSTEIN C SHOEMAKER AMSRD ARL WM T B BURNS AMSRD ARL WM TA W BRUCHEY M BURKINS W GILLICH B GOOCH T HAVEL E HORWATH M NORMANDIA J RUNYEON M ZOLTOSKI

NO. OF COPIES	ORGANIZATION
	AMSRD ARL WM TB P BAKER AMSRD ARL WM TC R COATES AMSRD ARL WM TD D DANDEKAR T HADUCH T MOYNIHAN M RAFTENBERG S SCHOENFELD T WEERASOORIYA AMSRD ARL WM TE A NIILER J POWELL

NO. OF COPIES	ORGANIZATION
1	LTD R MARTIN MERL TAMWORTH RD HERTFORD SG13 7DG UK
1	SMC SCOTLAND P W LAY DERA ROSYTH ROSYTH ROYAL DOCKYARD DUNFERMLINE FIFE KY 11 2XR UK
1	CIVIL AVIATION ADMINSTRATION T GOTTESMAN PO BOX 8 BEN GURION INTRNL AIRPORT LOD 70150 ISRAEL
1	AEROSPATIALE S ANDRE A BTE CC RTE MD132 316 ROUTE DE BAYONNE TOULOUSE 31060 FRANCE
1	DRA FORT HALSTEAD P N JONES SEVEN OAKS KENT TN 147BP UK
1	SWISS FEDERAL ARMAMENTS WKS W LANZ ALLMENDSTRASSE 86 3602 THUN SWITZERLAND
1	DYNAMEC RESEARCH LAB AKE PERSSON BOX 201 SE 151 23 SODERTALJE SWEDEN

NO. OF COPIES	ORGANIZATION
1	ISRAEL INST OF TECHLGY S BODNER FACULTY OF MECHANICAL ENGR HAIFA 3200 ISRAEL
1	DSTO WEAPONS SYSTEMS DIVISION N BURMAN RLLWS SALISBURY SOUTH AUSTRALIA 5108 AUSTRALIA
1	DEF RES ESTABLISHMENT VALCARTIER A DUPUIS 2459 BLVD PIE XI NORTH VALCARTIER QUEBEC CANADA PO BOX 8800 COURCELETTE GOA IRO QUEBEC CANADA
1	ECOLE POLYTECH J MANSON DMX LTC CH 1015 LAUSANNE SWITZERLAND
1	TNO DEFENSE RESEARCH R IJSSELSTEIN ACCOUNT DIRECTOR R&D ARMEE PO BOX 6006 2600 JA DELFT THE NETHERLANDS
2	FOA NATL DEFENSE RESEARCH ESTAB DIR DEPT OF WEAPONS & PROTECTION B JANZON R HOLMLIN S 172 90 STOCKHOLM SWEDEN

NO. OF
COPIES ORGANIZATION

COPIES	ORGANIZATION
2	DEFENSE TECH & PROC AGENCY GROUND I CREWTHER GENERAL HERZOG HAUS 3602 THUN SWITZERLAND
1	MINISTRY OF DEFENCE RAFAEL ARMAMENT DEVELOPMENT AUTH M MAYSELESS PO BOX 2250 HAIFA 31021 ISRAEL
1	TNO DEFENSE RESEARCH I H PASMAN POSTBUS 6006 2600 JA DELFT THE NETHERLANDS
1	B HIRSCH TACHKEMONY ST 6 NETAMUA 42611 ISRAEL
1	DEUTSCHE AEROSPACE AG DYNAMICS SYSTEMS M HELD PO BOX 1340 D 86523 SCHROBENHAUSEN GERMANY

INTENTIONALLY LEFT BLANK.